Evaluation of time-dependent grain-size populations for nucleation and growth kinetics

D. Crespo*
Departament de Física Aplicada, Universitat Politècnica de Catalunya, Campus Nord UPC, Mòdul B4, 08034 Barcelona, Spain

T. Pradell
Escola Universitària d'Enginyeria Tècnica Agricola, Universitat Politècnica de Catalunya, Urgell 187, 08020 Barcelona, Spain
(Received 5 December 1995; revised manuscript received 22 March 1996)

A theoretical calculation of time-dependent grain-size populations of an emerging phase driven by nucleation and growth kinetics is performed. A statistical *mean-field* model is presented for a completely degenerated system, based on the same assumptions as the Kolmogorov-Johnson–Mehl-Avrami (KJMA) model, that is to say, randomly distributed active nucleation sites which grow isotropically and collision resulting in a growth stop at the interface. Dependence of the kinetic parameters (nucleation and growth rates) on macroscopic and/or microscopic variables and on time is considered. The differential form of the KJMA model is applied to each grain-size population, providing a detailed microstructure development. As a result of this calculation, grain-size distributions are obtained. The validity of the model is tested by comparing the grain-size distributions obtained for a kinetically controlled process with a numerical Monte Carlo simulation. Imaging of the microstructure obtained by Monte Carlo is also shown. Finally, the model is computed with different kinetic conditions and the results are presented. [S0163-1829(96)06929-9]

I. INTRODUCTION

Most of the technologically interesting new materials are in a nonequilibrium state of condensed matter and their mechanical, magnetic, electric, thermal, and superconducting properties are essentially controlled by the presence of small particles. An optimized and controlled microstructure may be obtained by several methods, such as precipitation of a secondary phase from metastable systems under controlled conditions (i.e., temperature, pressure), or vapor deposition. Therefore, the emerging microstructure depends not only on the chemical composition but also on the mode of preparation and the previous history of the materials.

The knowledge of kinetics leading to a well defined microstructure is fundamental in order to obtain materials with the desired properties. The kinetics of first order phase transformation resulting in a microstructure formation is driven by nucleation and growth in most cases. Fluctuations promote cluster formation and dissolution until stable nuclei are formed, and further growth will give the final microstructure. Transforming systems may be characterized by the degeneracy parameter (p), which acounts for the number of distinct degenerate stable states into which the metastable phase transforms with equal probability. Nucleation may be homogeneous or heterogeneous, and time, temperature, or pressure dependent, giving a nucleation rate of $I(X,t)$, where X is any of the macroscopic variables which may influence the nucleation rate. Further growth of the nuclei may also be homogeneous, heterogeneous, diffusion controlled and also time, temperature, pressure, and grain-size dependent, giving a growth rate of $G(X,t)$.

Nucleation and growth kinetics in an infinite specimen, which results in the calculation of the volume fraction transformed at a given time, is well settled by Kolmogorov,[1] Johnson and Mehl,[2] and Avrami[3–5] (KJMA). This theory considers randomly distributed active nucleation sites which grow to form grains, and during the growing process may collide with other grains of neighboring sites, resulting in a growth stop at the interface. To summarize, let us define a control volume V_0 in which the growing phase occupies a volume $V(t)$; the transformed volume fraction is then $\xi(X,t)=V(t)/V_0$. Avrami introduced the concept of extended volume $\tilde{V}(t)$, as the volume that the growing grains would occupy if they were growing in isolation, establishing that

$$\frac{dV}{d\tilde{V}}=\frac{V_0-V}{V_0}. \tag{1.1}$$

This relation means that each grain has a probability of finding untransformed volume to continue growing equal to the probability of randomly finding untransformed volume in the whole volume. By integrating this equation we obtain

$$\ln[1-\xi(X,t)]=\frac{-\tilde{V}(t)}{V_0}. \tag{1.2}$$

Although some corrections to this approach have been suggested,[6] the KJMA theory is widely accepted and has been generalized for grains of arbitrary shape.[7–9] The main reason for this is that the theory itself is based only on statistical considerations, as has been recently pointed out by Cahn.[10]

The transformed volume fraction may be measured from differential scanning calorimetry (DSC) analysis, based on the construction of *T*-*T*-*T* (time-temperature-transformation) curves[11–13] and *T*-HR-*T* (temperature–heating rate–transformation) (Refs. 13–15) curves, or by other techniques. However, only the dependence of I and G on the controlled macroscopic parameters may be deduced from these measurements.

Further work on the kinetics of first order phase transitions has been devoted to the characterization and evaluation of correlation functions and their relationship with time-dependent diffraction studies. Sekimoto[16] evaluated an exact expression of the two-point correlation functions for arbitrary values of the degeneration parameter p, provided that the grain-size distribution is known, which is also related to the crystallized fraction. This correlation function has been related to the probability of magnetization greater than zero in a kinetic Ising model.[17]

The evaluation of the correlation functions in this system has usually been performed by means of the time-cone method. Axe and Yamada[18] obtained exact expressions of the autocorrelation function in the case of a one-dimensional system with $p\rightarrow\infty$ and constant I and G. In this case the universal grain-size distribution is obtained for $t\rightarrow\infty$. However, due to the lack of isotropy of the one-dimensional case, the results obtained here cannot be generalized to higher dimensions. Exact formal expressions of the correlation functions for a multiple-degenerate ground state in n dimensions were deduced by Ohta *et al.*[19] under certain restrictions; the most important of these is the fact that the growing rate must not be an increasing function of time.

Axe and Yamada also calculated the dependence of the x-ray-diffraction peak shape on the average radius $R(t)$ from scaling relations, finding that the peak intensity depends on $R(t)^5$, while the linewidth depends on $R(t)^{-1}$. These dependences indicate the main difficulties encountered in the evaluation of time-dependent microstructure development based on x-ray-diffraction peak broadening analysis.

There is a substantial difference between the two limits usually studied, namely the nondegenerate case ($p=1$) and the absolutely degenerate case ($p\rightarrow\infty$). In the nondegenerate case the notion of individual grains becomes nonsense as the transformed volume fraction increases, while in the degenerate case grains are distinguishable even after the transformation of the complete volume. Although the correlation functions can be evaluated in both cases, it is clear that they are much more useful in the nondegenerate than in the degenerate case, essentially because the concept of grain-size distribution is lost in the nondegenerate case. This is the situation in the study of ferromagnetic switching,[20–22] where the influence of the finite size of the nuclei has also been observed.[23] However, in the degenerate case the measure of the microstructure developed at various stages of the phase transformation may also make it possible to determine the dependence of the kinetic parameters on both microscopic and macroscopic variables. Several techniques have also been developed for obtaining the microstructure, either by obtaining images [i.e., transmission and scanning electron microscopy (TEM and SEM)],[24] or by indirect measurement [i.e., small angle scattering of x rays and neutrons (SAXS and SANS)].

This paper presents a theoretical calculation of time-dependent grain-size populations in a kinetically controlled process of nucleation and growth. The model is based on the same assumptions as the KJMA model, that is to say, randomly distributed active nucleation sites which grow isotropically and collide, resulting in a growth stop at the interface. The model calculates the grain-size populations as a function of $I(X,t)$ and $G(X,t)$ by defining the mean fraction of growing grains, and in this sense it is a kind of detailed integration of the KJMA theory. Theoretical dependence on any of the macroscopic and microscopic variables of the nucleation and growth rates is considered in the model. The model is less restrictive than previous work[19] and the obtained results can be used in the calculation of the correlation functions following Ref. 16.

The validity of the statistical model is tested by comparing the resulting grain-size populations with a Monte Carlo simulation for a kinetically controlled process. Some examples of the microstructure obtained by the Monte Carlo simulation are shown in a format equivalent to an SEM picture. Finally, grain-size distributions obtained under constant and variable nucleation and growth rates are presented, and their properties are discussed.

II. MODEL

A. Theoretical description

The evolution of grain populations with simultaneous nucleation and growth will be modeled in order to obtain grain-size distributions. In the proposed model the grains grow in a control volume V_0. The actual shape of this volume is not relevant, and for the sake of simplicity we will assume that it is cubic. We will assume that V_0 is large enough, that is to say $V_0^{1/3}$ is large compared with the average distance between grains $R_0=(G/I)^{1/4}$ in three dimensions.[16] This ensures that the system contains a sufficiently large number of grains to be self-averaging.

We will consider that ε is the initial radius of a nuclei. Next, let us define a typical length η related to the resolution available when looking at the sample. Therefore, we will suppose that a grain of radius r is distinguishable from another of radius $r+\eta$.

In order to work with dimensionless variables, a reduced coordinate system will be defined using η. Therefore, a reduced control volume will be defined as

$$v_0=\frac{V_0}{\eta^3} \tag{2.1}$$

and the reduced minimum grain size ϵ

$$\epsilon=\frac{\varepsilon}{\eta}. \tag{2.2}$$

A *variable* time scale $\tau(t)$ will also be defined considering that the growth ratio, $G(X,t)$, in dimensionless form has a value equal to unity. This can be achieved by setting the increase of the radius of a grain in a time interval $\tau(t)$ to be equal to the unit length η

$$\eta=\int_t^{t+\tau(t)} G(X,t')dt'. \tag{2.3}$$

Therefore, the nuclei will grow in time steps $\tau(t)$. With this assumption, an isolated grain having a dimensionless radius j at dimensionless time k will have a radius $j+1$ at time $k+1$. We have to emphasize the importance of the definition of this variable time scale because it supports the statistical properties of the populations on which the model is based.

Finally, we must define the dimensionless nucleation rate as

$$i(t)=\eta^3\int_t^{t+\tau(t)} I(X,t')dt'. \tag{2.4}$$

It is worth mentioning that we have explicitly suppressed the dependence of τ and i on X, because we consider that X are known functions of t, and the growing process may be parameterized only by the variable time. Moreover, due to the fact that we will always use unit time steps, we can write $\tau(t_k)$ and $i(t_k)$ in discrete form as τ_k and i_k, respectively.

Let $N_{j,k}$ be the population of grains of average radius r given by

$$j-1<r\leqslant j \tag{2.5}$$

at time t_k. The transformed dimensionless volume at time t_k may be written in terms of $N_{j,k}$ as

$$v_k=\sum_j N_{j,k}\frac{4}{3}\pi j^3. \tag{2.6}$$

Now we will define some extended populations $\tilde{N}_{j,k}$ in Avrami's sense, that is to say, those populations obtained while all the grains grow in isolation.

The number of nuclei which appear in a unit time step is different if we are considering the actual or the extended populations. Actual grains can only appear in the untransformed volume and then

$$N_{\rm new}(k)=i_k(v_0-v_k), \tag{2.7}$$

whereas the extended populations do not have this restriction, so

$$\tilde{N}_{\rm new}(k)=i_k v_0. \tag{2.8}$$

We base this statement on isotropic considerations. Each grain belonging to the extended populations grows as if it were completely isolated, and therefore does not use physical space. Consequently, a new nucleus can effectively appear inside the volume of any preexistent extended grain. On this point, we explicitly follow KJMA and leave aside the hypotheses of Ref. 6.

Accordingly with the previous assumptions, the appearing nuclei will belong to the populations $N_{\epsilon,k+1}$ and $\tilde{N}_{\epsilon,k+1}$. Simultaneously, the preexisting grains are growing. The evolution of the extended populations can be written as

$$\begin{aligned}\tilde{N}_{\epsilon,k+1}&=i_k v_0,\\ \tilde{N}_{j+1,k+1}&=\tilde{N}_{j,k},\quad j>\epsilon,\end{aligned} \tag{2.9}$$

considering that in our reduced system of variables, the growth rate is equal to unity.

To write similar equations for the evolution of the actual transformed populations we must include the fact that some grains of each population will grow at a reduced speed due to collisions with neighboring grains. Due to this, only a fraction α_k of each population will reach a radius large enough to migrate to the immediate population, so we have

$$\begin{aligned}N_{\epsilon,k+1}&=(1-\alpha_k)N_{\epsilon,k}+i_k(v_0-v_k),\\ N_{j+1,k+1}&=(1-\alpha_k)N_{j+1,k}+\alpha_k N_{j,k},\quad j>\epsilon.\end{aligned} \tag{2.10}$$

The introduction of the parameter α_k is the main point of the model. α_k is the probability that a grain has in its neighborhood sufficient untransformed volume to increase its radius. For this reason we have indexed α on k, because obviously α depends on time, but not on the grain radius because due to isotropic considerations the probability of finding untransformed volume is the same at each point of the control volume v_0.

The physical meaning of α_k is related to the mean growth rate $\overline{G(t_k)}$ of the grains. Axe and Yamada[18] have shown that it is possible to obtain approximate autocorrelation functions by integrating $\overline{G(t_k)}$. They observe, however, that the reason why this method gives inaccurate results is that $\overline{G(t_k)}$ do not correspond to any particular grain. In fact $\overline{G(t_k)}$ is a statistical value, and *must be* treated as a statistical property. So in our model the probability α_k is used in place of the mean growth rate $\overline{G(t_k)}$.

The above set of equations would offer us an iterative method for determining the populations $N_{j,k}$, provided that the value of α_k could be determined. This can be achieved by defining the extended volume in Avrami's sense—the volume that the grains would occupy if they were isolated—as

$$\tilde{v}_k=\sum_j \tilde{N}_{j,k}\frac{4}{3}\pi j^3 \tag{2.11}$$

and imposing that the transformed and extended volumes satisfy Avrami's relationship—Eq. (1.1)—at each iteration, which is written in our model as

$$\frac{v_{k+1}-v_{k-1}}{\tilde{v}_{k+1}-\tilde{v}_{k-1}}=\frac{v_0-v_k}{v_0}. \tag{2.12}$$

It is interesting to notice that none of these equations depend on the chosen value of v_0, as it is only used to determine the transformed volume fraction. Therefore, the evolution of the grain-size population can be simulated iteratively by successive computation of the system of Eqs. (2.9), (2.10), and (2.12), using an arbitrary value for v_0. It is also useful to define specific populations

$$n_{j,k}=N_{j,k}/v_0, \tag{2.13}$$

which are independent of the value v_0 used in the calculations.

The computation of the model is performed iteratively. The initial conditions of the populations are

$$\begin{aligned}n_{j,0}&=0,\quad j=1,M,\\ \tilde{n}_{j,0}&=0,\quad j=1,M,\end{aligned} \tag{2.14}$$

where M is the arbitrarily large number of populations simulated. At time step k, Eqs. (2.9) are computed giving the extended populations at time $k+1$. In fact, only the first

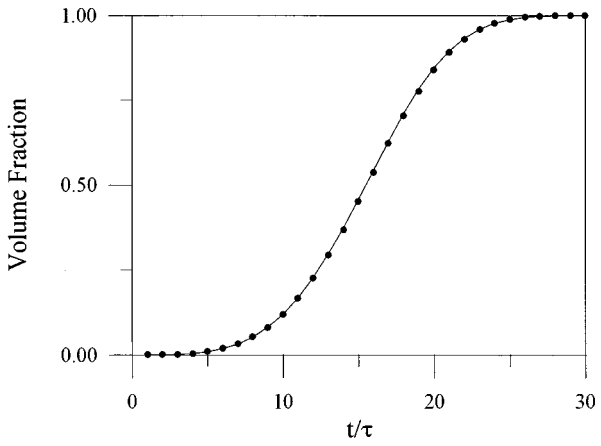

FIG. 1. Transformed volume fraction versus time for $i=10^5$ and $\epsilon=1$ measured in the Monte Carlo simulation (dots) and computed from the statistical model (continuous line).

$k+\epsilon$ extended populations are nonzero at time k; this means that the number M of simulated populations must be larger than $k+\epsilon$ or, more suitably, that the model can be integrated only while $k<M-\epsilon$.

Secondly, Eqs. (2.10) must be evaluated in order to obtain the true populations, but the value of α_k is still unknown. It is determined self-consistently by imposing the validity of (2.12). The first trial is performed by setting $\alpha_k=\alpha_{k-1}$, obtaining estimated values of $n_{j,k+1}$, and thus V_{k+1}. The true value of α_k is then determined by a Newton-Rapson method to an accuracy of 10^{-10}. The process is repeated until the untransformed volume fraction becomes negligible, typically 10^{-3}.

Under the above conditions computer time and memory storage needed for the integration are negligible. Due to its flexibility, it is possible to obtain the grain-size distribution as a function of time for any nucleation process, provided that the dependence of $G(X,t)$ and $I(X,t)$ is previously known. For the simplest case, with constant $G(X,t)$ and $I(X,t)$, the time step τ_k and the reduced nucleation rate i_k are also constant.

B. Comparison with a Monte Carlo simulation

We have tested the validity of the model presented against a Monte Carlo simulation in the simplest case of constant $G(X,t)$ and $I(X,t)$. The nucleation sites are chosen randomly and the subsequent constant-speed growth of the nuclei is stopped only by collision with neighboring grains. This was performed in a 256^3 lattice with periodic boundary conditions. In order to obtain acceptable statistics the simulation was performed 32 times and the populations obtained were averaged. On an HP9000/720 workstation the whole process consumed about 10 h of CPU time and 40 Mb of RAM storage for the chosen values of the parameters.

Figure 1 shows the dependence of volume fraction on time for $i=10^5$ and $\epsilon=1$, showing an excellent agreement between our model and the Monte Carlo simulation. The value of ϵ was chosen equal to unity due to the limitations of the Monte Carlo procedure; in fact with greater values of ϵ the volume occupied by the nuclei just after nucleation is an appreciable fraction of the total lattice volume, so Monte Carlo results are affected by the lattice dimensions. The only way to solve this problem is to increase the size of the lattice, but then the amount of RAM storage needed becomes prohibitive.

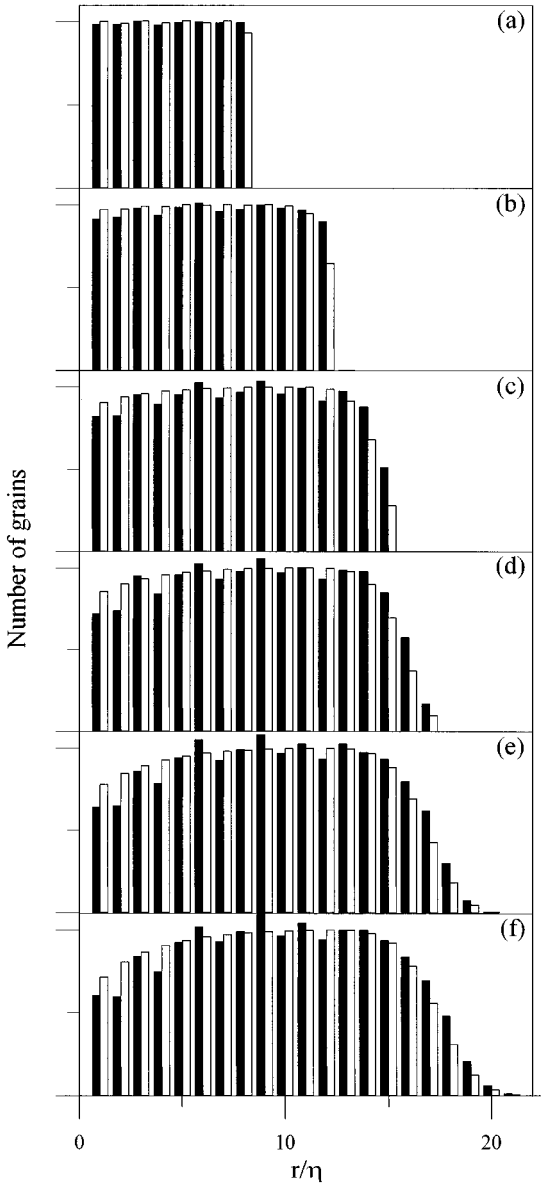

FIG. 2. Bulk grain-size distribution measured in the Monte Carlo simulation (black bars) and computed from the statistical model (white bars) for transformed volume fractions: (a) 5%, (b) 20%, (c) 40%, (d) 60%, (e) 80%, and (f) 95%. Vertical scale is the same in all the plots.

It is important to notice that the volume fraction calculated by the Monte Carlo method coincides with the integration of the KJMA equation—Eq. (1.2)—within an accuracy of 10^{-3}, which confirms the validity of our assumption in Eq. (2.8).

Figure 2 shows the bulk grain-size distribution in both cases for several different transformed volume fractions; again the agreement between the two methods is excellent. It is important to notice that the scale used for the volume populations is the same for both methods, showing that the

statistical model is quantitatively exact. Therefore, our assumption that the KJMA theory in differential form is applicable not only to the whole transformed volume but also to each grain-size population is correct.

III. RELATIONSHIP WITH MEASURED SURFACE POPULATIONS

The final goal of our work is to offer a tool which allows us to compare the statistical predictions with results obtained from image analysis of experimental data obtained by any microscopic technique. In the case of SEM analysis and also of TEM analysis of a negligible thickness sample, the observation of the sample is performed over a surface cut. Although it is well known that the total surface and volume fraction of the transformed phase are the same,[25] this equality is not preserved for each population, thus giving different bulk and surface grain-size distributions. In other words, we will not observe the actual populations but their surface tracks. This problem has been studied by different authors showing that the surface distribution obtained is highly dependent on the shape of the individual grains. In our model the grains are assumed to be always spherical, a situation which was studied by Saltykov.[26]

A grain will be cut at an unknown random distance y from its center, so we have to average between all the possibilities in order to obtain the true grain-size distribution.

Let us study a grain of radius R which is cut by a plane; due to symmetry the probability of cutting the grain through the upper half sphere is the same as through the lower half, and so it is sufficient to calculate the average radius of the circle obtained when cutting the upper half sphere. In particular, this means that a grain whose center is at a distance δ over the cutting plane shows the same section as one whose center is at the same distance δ below the cutting plane.

Let y be the distance between the cutting plane and the center of the grain; therefore, the radius of the resulting circle r will satisfy

$$r=\sqrt{R^2-y^2}, \tag{3.1}$$

y being a random variable, with constant probability density $p(y)$,

$$p(y)=\frac{1}{R} \tag{3.2}$$

and by imposing the condition of probability conservation

$$p(y)dy=p(r)dr, \tag{3.3}$$

we can determine the probability density function $p(r)$

$$p(r)=p(y)\left|\frac{dy}{dr}\right|=\frac{1}{R}\left|\frac{dy}{dr}\right|. \tag{3.4}$$

The probability of having a value of r between r_1 and r_2 is

$$p(r_1\leqslant r\leqslant r_2)=\int_{r_1}^{r_2}\frac{1}{R}\left|\frac{dy}{dr}\right|dr=\frac{1}{R}|y(r_2)-y(r_1)|$$

$$=\frac{1}{R}\left|\sqrt{R^2-r_2^2}-\sqrt{R^2-r_1^2}\right|. \tag{3.5}$$

We must discretize this probability because our populations are discrete, so writing $r_1=r-1$ and $r_2=r$ we have

$$p(r-1\leqslant\rho\leqslant r)=p_1(r,R)=\frac{1}{R}(\sqrt{R^2-(r-1)^2}-\sqrt{R^2-r^2}). \tag{3.6}$$

To obtain the observed grain distribution $N_{j,k}^l$ of radius j due to the population $n_{l,k}$ we must multiply $p_1(r,R)$ by the probability of cutting any of the grains of this population. This probability is the product of the value of $n_{l,k}$, the diameter of the population $2l$ and the surface S of the sample considered, so we have

$$N_{j,k}^l=2lSn_{l,k}p_1(j,l)=2S(\sqrt{l^2-(j-1)^2}-\sqrt{l^2-j^2})n_{l,k} \tag{3.7}$$

and the observed population of radius j is obtained by adding $N_{j,k}^l$ over all the possible values of l

$$N_{j,k}=2S\sum_{l=j}^{\infty}(\sqrt{l^2-(j-1)^2}-\sqrt{l^2-j^2})n_{l,k}. \tag{3.8}$$

As the actual shape of the grains is not spherical, Eq. (3.8) is only an approximation whose validity must be tested by comparison with the Monte Carlo simulation. Therefore, Eq. (3.8) has been applied to the populations obtained with our model, and compared with the average grain-size distribution determined over a surface cut in the Monte Carlo simulation. In order to obtain a reasonable statistic for each grain population, 10 planes were randomly chosen in each Monte Carlo simulation and the size distribution was determined for each of them. Figure 3 shows an example of one of the chosen planes. In this calculation two assumptions were taken. First we did not join contiguous grains, thus assuming that the total number of grains remain unchanged. Second, an *effective* radius r was given to each grain, corresponding to a circle of equivalent surface S_e, that is

$$r=\sqrt{\frac{S_e}{\pi}}. \tag{3.9}$$

Figure 4 shows the comparison between the measured (Monte Carlo) and computed (statistical) resulting distributions. For the different values of the transformed volume fraction, and again using the same scale for both populations, the quantitative agreement is excellent. The main difference is that small grain-size populations are slightly underestimated in the statistical model due to the fact that grains are not spherical, as considered in Eq. (3.8).

The shape of the distributions obtained agrees with the highly accurate TEM experimentally measured microstructure of a partially crystallized FINEMET material.[24]

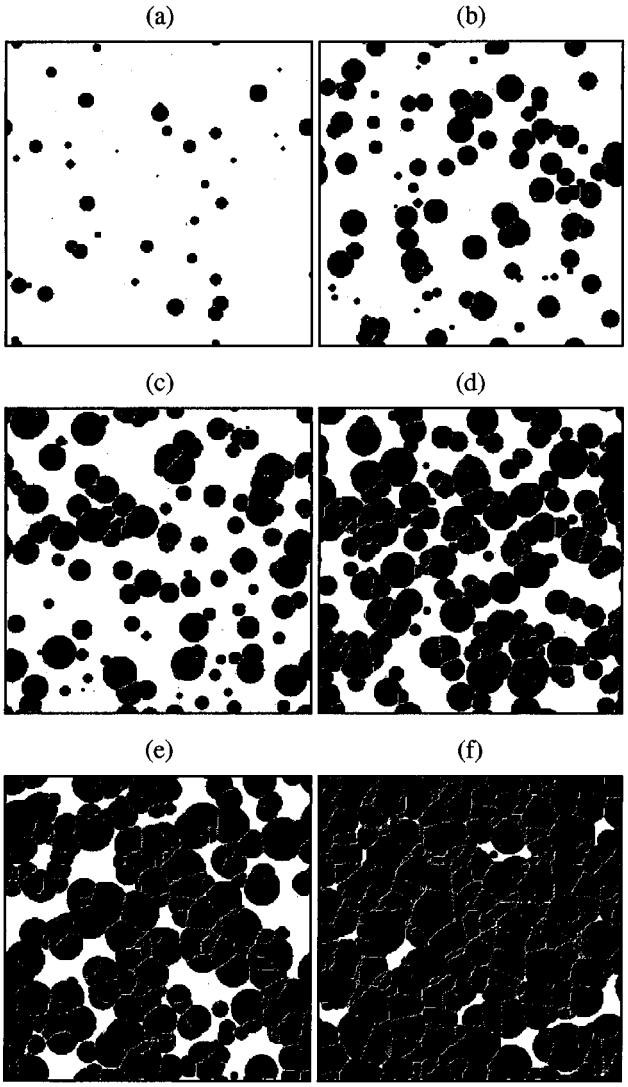

FIG. 3. Randomly chosen section of a Monte Carlo simulation, equivalent to a SEM micrograph, for transformed volume fractions: (a) 5%, (b) 20%, (c) 40%, (d) 60%, (e) 80%, and (f) 95%. Grains are shown in dark and untransformed volume in white.

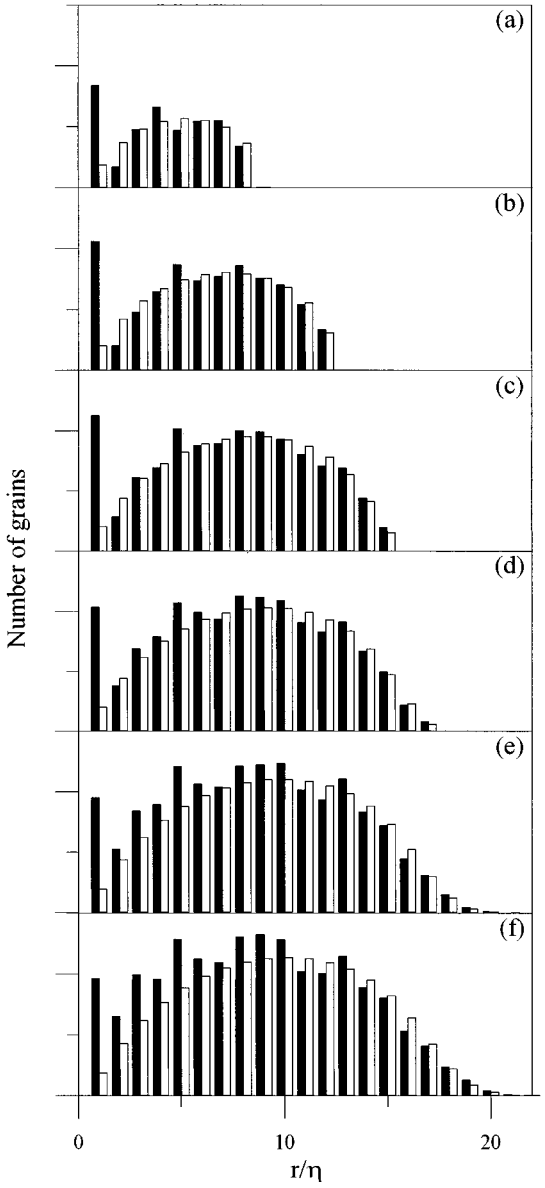

FIG. 4. Average surface grain-size distribution measured in the Monte Carlo simulation and computed from the statistical model and Eq. (3.8). Transformed volume fractions are (a) 5%, (b) 20%, (c) 40%, (d) 60%, (e) 80%, and (f) 95%.

IV. APPLICATIONS

The statistical model presented here allows us to explore a wide range of parameters and to compare the results with experimentally measured grain-size distributions, thus determining indirectly the value of the interesting kinetic parameters. Next, we will present the results of the integrations of the statistical model under different kinetic conditions.

A. Constant nucleation rate

The transformation at a constant nucleation rate corresponds to a physical situation that is difficult to obtain, because the desired constant conditions usually need some time to be set up and the effect of this transient procedure cannot be ignored. However, it can be used as a test by comparing with the general results obtained by existing theories.

Figure 5 shows the bulk grain-size distribution at increasing transformed volume fractions for $\epsilon=1$ and three values of the nucleation rate i. The shape of the distributions after adequate scaling is very close, showing the expected universal behavior.[18] The natural length and time scales for this system are $\eta_n=(I/G)^{-1/4}$ and $\tau_n=(IG^3)^{-1/4}$, which indicate that the average grain-size should scale as $I^{-1/4}$. The average radius obtained has been fitted to a power law $\langle r\rangle=ki^{\beta}$ in which k depends on the transformed volume fraction, giving a value of $\beta=-0.2445$ with a coefficient of determination of 0.9997, and thus showing excellent agreement with the above statement.

The main differences between the three plots in Fig. 5 are in the shape of the grain-size distribution at large radius. Larger dispersion around the mean values is obtained for decreasing nucleation ratios due to the fact that grains are growing for long periods, thus allowing larger dispersion around the mean value for each population.

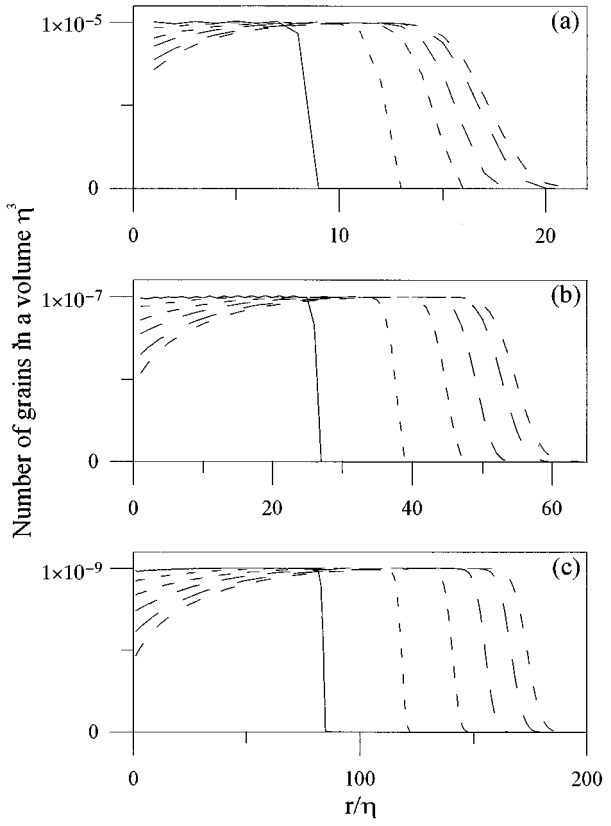

FIG. 5. Grain-size distributions obtained with $\epsilon=1$ and (a) $I=10^{-5}$, (b) $I=10^{-7}$, and (c) $I=10^{-9}$, plotted for transformed volume fractions of 5%, 20%, 40%, 60%, 80%, and 95%. The solid line in the plots corresponds to the lower volume fraction.

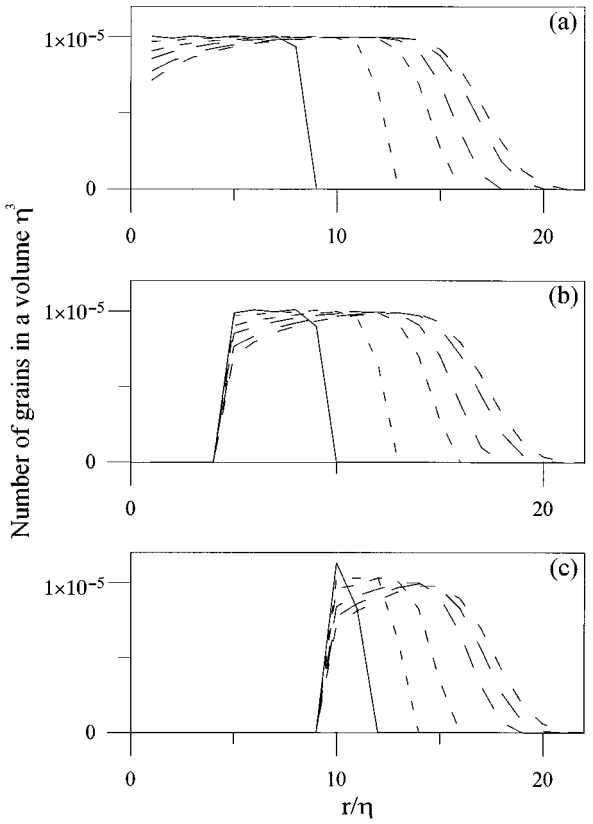

FIG. 6. Grain-size distributions obtained with $I=10^{-5}$ and (a) $\epsilon=1$, (b) $\epsilon=5$, and (c) $\epsilon=10$, plotted for transformed volume fractions of 5%, 20%, 40%, 60%, 80%, and 95%. The solid line in the plots corresponds to the lower volume fraction.

Figure 6 shows the dependence of the grain-size distribution on ϵ; now the width of the grain-size distribution becomes smaller as ϵ increases, due to the restriction of the whole volume. This figure shows that for a given value of I the statistical method may give inaccurate results if the chosen value for η is too small in relation with ε.

The results obtained with this method must be interpreted with care, due to the dimensionless parameters employed. Thus, as η is used in the definition of the reduced nucleation rate i, a change in the value of ϵ in a specific problem involves an implicit change in the value of i. Moreover, the chosen value of η establishes the uncertainty in the determination of the critical nucleation radius ϵ.

B. Variable nucleation rate

The potential of the statistical model presented here is that a more realistic procedure for grain development may be easily analyzed. The dependence of I and G in any macroscopic variable dependent on time may be introduced by determining the value of $i(t)$ and the appropriate time scale for modeling the growth process. As an example of the applicability of the statistical model, we have studied a heat treatment of a typical amorphous material which undergoes a nanocrystalline structure in a selected range of temperatures.[27] The kinetic parameters of the material are shown in Fig. 7.

The treatment considered consists of a constant heating rate from room temperature (300 K) to 780 K and a subsequent constant cooling rate again to room temperature. We have studied two possible processes: the first, labeled (a), heating at a constant rate of $1\ \mathrm{K\,s^{-1}}$ and cooling at a rate of $0.2\ \mathrm{K\,s^{-1}}$; and the opposite to it, labeled (b), heating at a constant rate of $0.2\ \mathrm{K\,s^{-1}}$ and cooling at a rate of $1\ \mathrm{K\,s^{-1}}$. The values chosen for η and ε were 1 and 5 nm, respectively.

The first difference between the two procedures arises from the fact that the crystallized volume fraction is different

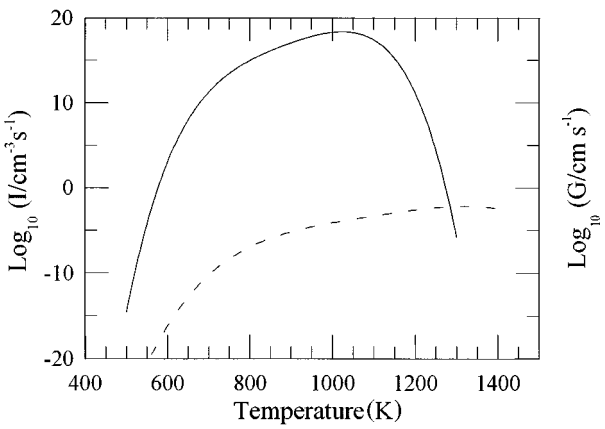

FIG. 7. Logarithmic plot of $I(T)$ (continuous line) and $G(T)$ (dashed line) used in Sec. IV B, after Ref. 27.

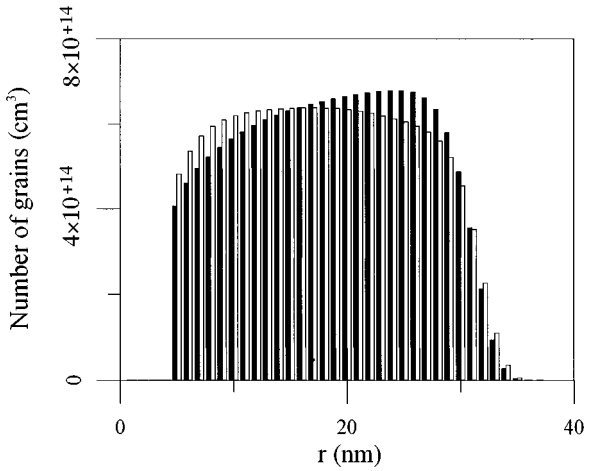

FIG. 8. Bulk grain-size distribution obtained with the statistical model after processes (a) (black bars) and (b) (white bars) in Sec. IV B. See text for details.

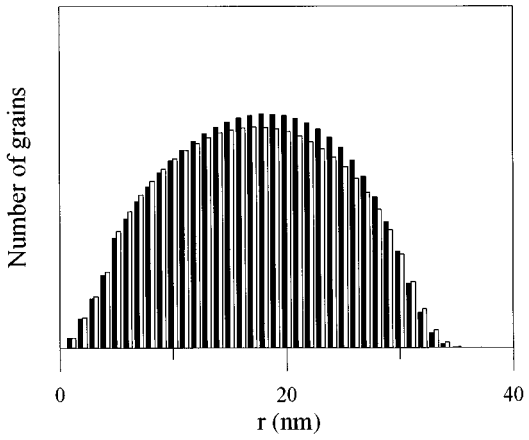

FIG. 9. Surface grain-size distribution computed from the statistical model after processes (a) (black bars) and (b) (white bars) in Sec. IV B.

after the two treatments. The computed crystallized volume fractions are 66.0% and 62.1%, respectively. Moreover, the final grain-size distribution is different in the two cases, as can be seen in Fig. 8: treatment (a) results in an average grain-size of 18.6 nm, while treatment (b) gives an average grain-size of 18.0 nm, with a 3% difference. Finally, the shape of the two grain-size distributions reflects the importance of the thermal history, because nucleation must precede any crystal growth.

The calculated surface grain-size distributions are shown in Fig. 9. Differences are also visible here, although they are less evident due to the fact that each bulk population contributes to all surface populations of a smaller radius.

V. CONCLUSIONS

A mean field model for evaluating grain-size populations of a completely degenerated system with a nucleation and growth kinetics has been developed. The main assumptions are the same as those established by the KJMA model for isotropic growth, considering that new nuclei can only appear and grow in the untransformed volume, whereas this restriction is not imposed on the extended populations. The differential form of the KJMA equation is applied in order to determine the average fraction of growing grains as a function of time. This parameter is used to calculate the evolution of each grain-size population.

A Monte Carlo simulation has been performed and some pictures of the microstructure obtained are shown. The grain-size populations and the transformed volume fractions calculated by this simulation completely agree with the ones obtained by the statistical model using the same kinetic parameters, confirming the applicability of the KJMA model for the discrete populations. As a consequence, the statistical model predicts the final specific grain-size populations from given kinetic parameters.

The practical importance of the statistical model presented here comes from the fact that even in the simplest case of constant nucleation and growth rates its computation time is a negligible fraction of the time needed by an equivalent Monte Carlo simulation. Moreover, it allows complex processes to be studied due to its ability to include variable nucleation and growth rates without increasing the computing time. The spatial correlation functions are easily calculable, thus allowing comparison of the results obtained with experimental data from x-ray-diffraction analysis and similar techniques.

Grain-size populations measured experimentally by any direct imaging technique are different from the calculated ones because of the geometry of the sample preparation. A method for calculating the actual populations from experimentally measured ones is also used. Therefore, in the present study a method for evaluating the kinetic parameters—nucleation and growth rates—directly from the measured grain-size populations is given.

The definition of a reduced variable time scale allows the evolution of grain populations to be modeled under varying external conditions, thus offering a powerful method for simulating true grain growth protocols.

ACKNOWLEDGMENTS

The authors are indebted to N. Clavaguera and M.T. Clavaguera-Mora, who suggested the subject and revised the manuscript, and also for many very stimulating discussions. This work was financed by DGICYT Grant No. PB94-1209, UPC Grant No. PR9505, and CICYT Grant No. MAT96-0692.

*Electronic address: crespo@benard.fa.upc.es

[1] A. N. Kolmogorov, Bull. Acad. Sci. USSR, Phys. Ser. **1**, 355 (1937).
[2] W. A. Johnson and P. A. Mehl, Trans. Am. Inst. Min. Metall. Eng. **135**, 416 (1939).
[3] M. Avrami, J. Chem. Phys. **7**, 1103 (1939).
[4] M. Avrami, J. Chem. Phys. **8**, 212 (1940).
[5] M. Avrami, J. Chem. Phys. **9**, 177 (1941).
[6] V. Erukhimovitch and J. Baram, Phys. Rev. B **50**, 5854 (1994).
[7] K. Sekimoto, Phys. Lett. **105A**, 390 (1984).
[8] K. Sekimoto, Physica A **135**, 328 (1986).
[9] K. Sekimoto, Int. J. Mod. Phys. B **5**, 1843 (1991).

[10] J. W. Cahn, *Thermodynamics and Kinetics of Phase Transformations*, MRS Symposia Proceedings No. 398 (Materials Research Society, Pittsburgh, PA, 1996).
[11] D. R. Uhlmann, J. Non-Cryst. Solids **7**, 337 (1972).
[12] P. I. K. Onorato, D. R. Uhlmann, and R. W. Hopper, J. Non-Cryst. Solids **41**, 189 (1980).
[13] N. Clavaguera, J. Non-Cryst. Solids **162**, 40 (1993).
[14] N. Clavaguera and J. A. Diego, Intermetallics **1**, 187 (1993).
[15] N. Clavaguera and M. T. Clavaguera-Mora, Mater. Sci. Eng. A **179**, 288 (1994); **1**, 187 (1993).
[16] K. Sekimoto, J. Phys. Soc. Jpn. **53**, 2545 (1984).
[17] H. L. Richards, S. W. Sides, P. A. Rikvold, and M. A. Novotny, J. Magn. Magn. Mater. **150**, 37 (1995).
[18] J. D. Axe and Y. Yamada, Phys. Rev. B **34**, 1599 (1986).
[19] S. Ohta, T. Ohta, and K. Kawasaki, Physica A **140**, 478 (1987).
[20] H. Tomita and S. Miyashita, Phys. Rev. B **46**, 8886 (1992).
[21] P. A. Rikvold, H. Tomita, S. Miyashita, and S. W. Sides, Phys. Rev. E **49**, 5080 (1994).
[22] P. D. Beale, Integrat. Ferroelectrics **4**, 107 (1994).
[23] H. M. Duiker and P. D. Beale, Phys. Rev. B **41**, 490 (1990).
[24] U. Köster, U. Schünemann, M. Blank-Bewersdorff, S. Brauer, M. Sutton, and G. B. Stephenson, Mater. Sci. Eng. A **133**, 611 (1991).
[25] E. E. Underwood, *Quantitative Stereology* (Addison-Wesley, Reading, MA, 1970), p. 25.
[26] S. A. Saltykov, *Stereology* (Springer-Verlag, New York, 1967), p. 163.
[27] N. Clavaguera, T. Pradell, J. Zhu, and M. T. Clavaguera-Mora, Nanostruct. Mat. **6**, 453 (1995).